Volcanoes, Landscapes, and Structures in and near Flagstaff, Arizona: Field Guide for a One-Day Excursion

R.F. Holm

CONTRIBUTED REPORT CR-22-F

November 2022

Arizona Geological Survey

azgs.arizona.edu | repository.azgs.az.gov

UA Science

Arizona Geological Survey

P.A. Pearthree, Arizona State Geologist and Director

Manuscript approved for publication in November 2022
Printed by the Arizona Geological Survey
All rights reserved

To retrieve an electronic copy of this publication: www.repository.azgs.az.gov

For information on the mission, objectives or geologic products of the Arizona Geological Survey visit azgs.arizona.edu

This publication was prepared by the Arizona Geological Survey at the University of Arizona. The University of Arizona, or any department thereof, or any of their employees, makes no warranty, expressed or implied, or assumes any legal liability or responsibility for the accuracy, completeness, or usefulness of any information, apparatus, product, or process disclosed in this report. Any use of trade, product, or firm names in this publication is for descriptive purposes only and does not imply endorsement by the University of Arizona.

The AZGS Contributed Report series provides non-AZGS authors with a forum for publishing documents concerning Arizona geology. While review comments may have been incorporated, this document does not necessarily conform to AZGS technical, editorial, or policy standards.The Arizona Geological Survey issues no warranty, expressed or implied, regarding the suitability of this product for a particular use. Moreover, the Arizona Geological Survey shall not be liable under any circumstances for any direct, indirect, special, incidental, or consequential damages with respect to claims by users of this product. The author(s) is solely responsible for the data and ideas expressed herein.

Recommended Citation. Holm, R.F., 2022, Volcanoes, Landscapes, and Structures in and near Flagstaff, Arizona: Field Guide For a One-Day Excursion. Arizona Geological Survey Contributed Report CR-22-F, 22 p.

Cover Photo: Aerial photo of Sunset Crater (foreground) and San Francisco Mountain (middle ground) of the San Francisco volcanic field of northern Arizona. Photo by Ted Grussing.

UA SCIENCE
ARIZONA GEOLOGICAL SURVEY
Geosciences serving Arizona since 1887

Volcanoes, Landscapes, and Structures In And Near Flagstaff, Arizona: Field Guide For A One-Day Excursion

2022

Richard F. Holm

This one-day field trip takes participants to outcrops and vantage points to see young (6.0-0.001 **Ma**) eruption products in the San Francisco volcanic field. Included are cinder cones, lava domes, and a composite volcano, and basalt, andesite, and dacite lava flows. Discussions cover mechanisms of volcanic eruptions, growth and collapse of volcanoes, and evolution of southern Colorado Plateau landscapes where regional structures guide stream and volcanic systems.

Words in bold or bold and underlined are defined in Glossary. Supplemental photographs are in Appendix A. A suggested schedule for a one-day trip is in Appendix B.

INTRODUCTION

The region around Flagstaff is the largest young volcanic province in Arizona (Fig 1). The sector containing San Francisco Mountain is named the San Francisco volcanic field. This field covers eroded Permian and Triassic sedimentary rocks on the southern margin of the Colorado Plateau with more than 2,000 mi^2 of lava flows, volcanoes, and cinder blankets. Some lava flows from vents on the Plateau drape over the Mogollon Rim into the Transition Zone. In the volcanic field are more than 800 small volcanoes, including cinder cones, lava domes, and tuff rings. Six large clusters of lava domes and flows, four shield volcanoes, and one composite volcano stand out in landscape views.

Volcanic rocks classified with hand-specimen **petrography,** and some of their distinguishing features, are listed left to right in Table 1 in order of decreasing abundance in the volcanic field.

Table 1. Common Volcanic Rocks

	basalt	**andesite**	**dacite**	**rhyolite**
silica	45 wt. %	increases to		75 wt. %
alkali	3 “	increases to		9 “
iron	12 “	decreases to		2 “
color	black/dk gray	grey to pink		white
viscosity	low	medium		high
lava temp.	1150ºC	decreases to		750ºC
large crystals	olivine pyroxene	pyroxene plagioclase	plagioclase hornblende	quartz sanidine

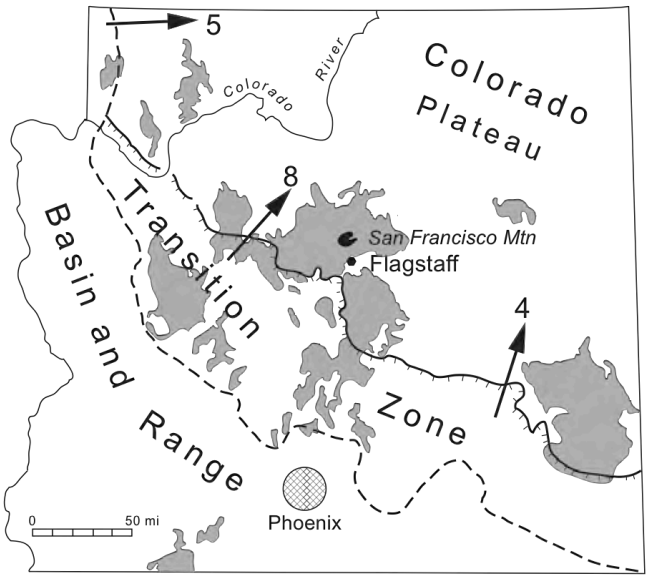

Figure 1. Upper Cenozoic volcanic rocks (gray) are widespread in northern and central Arizona. Arrows show progression of basaltic volcanism from the Arizona Transition Zone onto the Colorado Plateau in km/m.y. since middle Miocene (Crow et al., 2011). Thick line with tick marks is Mogollon Rim, the southwestern edge of the Colorado Plateau.

The field trip follows a route through the central and eastern San Francisco volcanic field (Fig. 2). In this part of the volcanic field the courses of most streams and the flow directions of many lavas trend northeast down the eroded **dip slope** of the Kaibab (Lower Permian) and Moenkopi (Lower to Middle Triassic) formations. The elongated lava flows give the north and east sides of the volcanic field a digital appearance (Fig. 2).

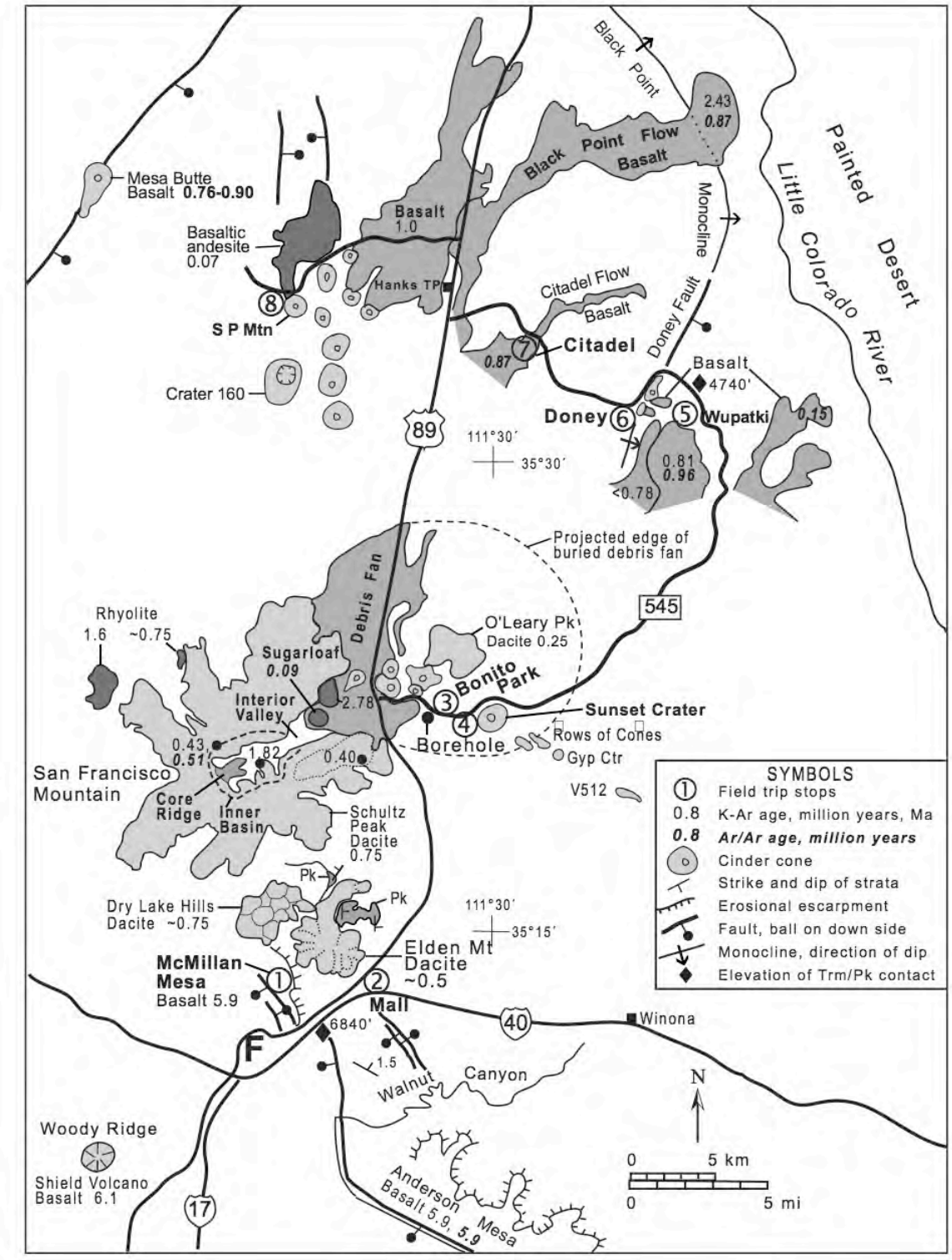

Figure 2. Map showing field trip route and stops, and selected geologic features in the central and eastern San Francisco volcanic field; map based on Ulrich et al., 1984. Trm: Moenkopi Formation, Lower and Middle Triassic, sandstone and siltstone; Pk: Kaibab \Formation, Lower Permian, dolostone and limestone. K-Ar dates from Damon et al., 1974, McKee, et al., 1998, and Reynolds et al., 1986. Ar-Ar dates from Conway et al., 1997, Morgan et al., 2010, Hanson, 2010, Karatson et al., 2010, Ben-Horin et al., 2021. Ma is million years.

FIELD TRIP DESCRIPTION

Miles measured on Google Earth.
F*rom the downtown intersection of Humphreys Street and Historic Route 66/ Santa Fe Ave. –**F** on Figure 2 --drive east on Route 66 1.0 mi (left lane).*
Turn left at 4th signal onto Switzer Canyon Drive. Go 0.58 mi to roundabout.
At roundabout turn right onto Turquoise Drive. Go 0.7 mi to Forest Avenue at signal.
Turn right at signal onto Forest Ave. Go 0.63 mi to N. Gemini Drive.
Turn left at signal onto N. Gemini Dive. Go 0.3 mi to entrance to Buffalo Park.
Park on right just before entry to the Park.

Gray to tan Kaibab Formation crops out in south Flagstaff and on the NAU campus. Red Moenkopi Formation is on the north side of east Route 66. Switzer Canyon Drive and Turquoise Drive follow a **graben** on the west side of McMillan Mesa. Forest Avenue cuts through the fault scarp and climbs to the top of the mesa.

Take the trail around the south side of the green water tank and then right on the social trail by the chain-link fence to lava outcrop on edge of mesa, about 1,400 feet (570 feet beyond bend in fence). Be alert for cactus, open cracks of **columnar joints**, and deep fractures by cliff edge.

Stop 1. McMillan Mesa. McMillan Mesa is capped by the oldest lava flow in the Flagstaff area (Fig. 2, 5.9 **Ma**). The Late Miocene basalt (SiO_2=49.9) extruded from the Woody Ridge shield volcano southwest of Flagstaff (Fig. 2), and spread northeast as a thin sheet on eroded Permian and Triassic strata (Holm, 2001a). The lava flowed into a northwest-trending **strike valley** that was bound on the southwest side by a dip slope on the Kaibab Formation and on the northeast side by a **cuesta** of Shinarump Conglomerate (Fig. 3). Quartzite and chert pebbles eroded from the

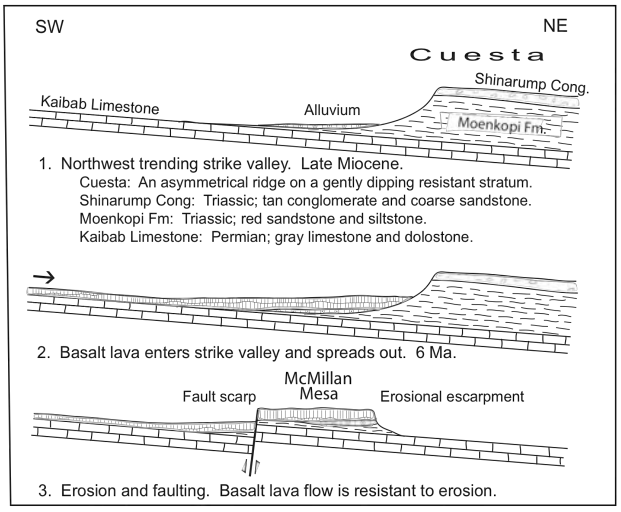

Figure 3. Sequence of events that formed McMillan Mesa. Events are also applicable to Anderson Mesa.

Shinarump cuesta occur abundantly under the basalt, and sparsely on its surface.

Today, the Shinarump Conglomerate crops out near and along the Little Colorado River (Fig. 2). Erosional retreat of the cuesta down-dip since 5.9 Ma has been 7-8 km/**m.y.**

Seen to the southeast are Anderson Mesa, capped by horizontal basalt lava flows (5.9 Ma), and Mormon Mountain, a cluster of dacite lava domes (3.1 Ma) (Fig. 4). The Anderson Mesa basalt erupted from a shield volcano about six miles southeast of Mormon Mountain. An intravalley divide on the Moenkopi Formation in the northwest-trending strike valley kept the lavas on McMillan and Anderson mesas from merging. Because the intravalley divide was not protected by lava it was susceptible to erosion, and Walnut Creek eventually eroded Walnut Canyon in the low area between the two lava-capped mesas (Fig. 2).

Below the horizontal surface of Anderson Mesa the tops of Ponderosa pine trees in the gap between the two mesas are parallel to the erosion-stripped northeast dip slope (1.5º) on the Kaibab Formation (Fig. 4).

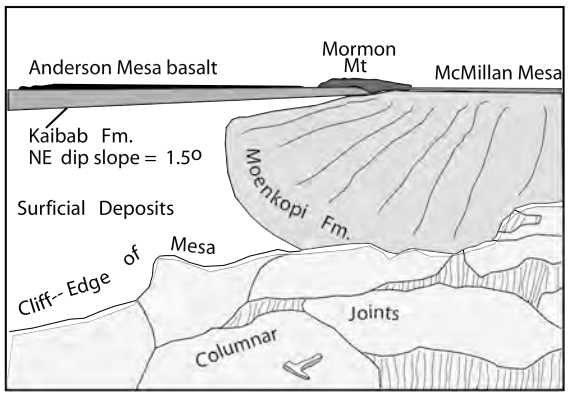

Figure 4. Sketch of view looking southeast from Stop 1 on basalt lava at the east edge of McMillan Mesa.

In downtown Flagstaff the Moenkopi Formation-Kaibab Formation contact is at elevation 6840 feet. Near the Wupatki National Monument visitor center (Stop 5, 27 miles northeast of Flagstaff) the same contact is at elevation 4740 feet (Fig. 2). The apparent dip between these locations is 0.83º.

After faulting and erosion formed McMillan Mesa its northern end was covered by Dry Lake Hills (~0.75 Ma, SiO_2=62.21), a cluster of eight dacite lava domes (Fig. 2). The domes are aligned on the projections of northwest-trending faults (Fig. 2).

Elden Mountain erupted later on the eroded Kaibab Formation east of McMillan Mesa as a composite lava dome of dacite (Fig. 2, ~0.5 Ma, SiO_2=66.39). Numerous thick bulbous flows radiate from several summit vents. Different internal structures and eruption mechanisms of lava domes are illustrated in Figure 5. Dry Lake Hills contain both endogenous and exogenous lava domes.

The different shapes of the basalt sheet flows and the rhyolite and dacite lava domes are due to different viscosities of the lavas, which result principally from different silica contents and temperatures (Table 1).

Features of very low viscosity of the basalt sheet lava include: low aspect ratio (thickness÷length), rubble-free tops and bottoms of **flow units**,

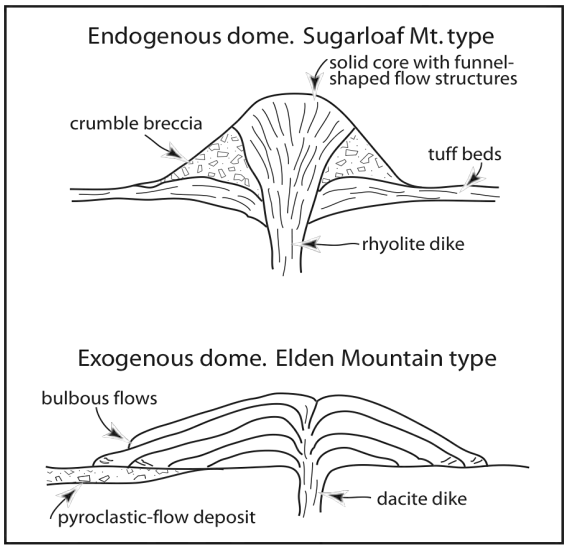

Figure 5. Lava domes. Endogenous domes push up and inflate on the inside. Exogenous domes are layered from summit vents; the fronts of flows have inward dipping ramping shear fractures.

holocrystalline internal texture, and **vesicle cylinders** and **vesicle sheets** (see in detached block at north end of outcrop--**be careful at cliff edge**); these features and locally preserved ropy and festoon surface structures indicate the lavas are **pahoehoe** flows.

The lava domes, in contrast, are steep sided, the flows are short and thick, and the aspect ratio is high. The youngest flow on the southeast side of Elden Mountain was so stiff that it stopped flowing before it reach the base of the volcano (see at Stop 2).

On return to parking lot, a gap in the basalt cliff by the bend in the chain-link fence allows access to a **colluvium**-covered slope below the lava that contains Shinarump pebbles.

The route to Stop 2 is down the northeast erosional escarpment of McMillan Mesa; red sandstone of the Moenkopi Formation is on the left. At the bottom of the escarpment Cedar Avenue passes onto eroded Kaibab Formation.

*Return to Forest Ave. Turn left at signal. Road now named Cedar Ave., left lane. Stay on Cedar Ave. to 2nd signal at 4th St, middle lane, small jog left then straight ahead on Lockett Ave. for 1.0 mi to Fanning Drive at 2nd stop sign. (**Lockett is posted for 25 mph**). Turn right onto Fanning Dr., continue on Fanning for 0.18 mi to signal at Route 66. (left lane)*
Turn left onto Route 66 (Santa Fe Ave), go through 2 signals, get in right lane.
After 0.84 mi turn right at 3rd signal at Cummings St. into Flagstaff Mall; park in front of JC Penney. Stop 2.

Stop 2. Flagstaff Mall. Prominent on the southeast side of Elden Mountain are overlapping lava flows. The lowest flow has subhorizontal benches related to ramping shear fractures that dip inward toward the source of the flow (Fig. 5). These structures formed when the front of the lava flow reached the base of the volcano, flowed onto flatter ground, and slowed down. Trailing lava then overrode the slower moving front.

The top flow has vertical longitudinal joints that formed when the lava spread laterally as it advanced down slope and adjusted its shape to the surface of the underlying flow.

Elsewhere on Elden Mountain, flows that advanced onto flat ground beyond the base of the volcano have conjugate joints that formed as the lava spread out (two sets of joints intersect at high angle).

These regular fractures result from gravity-driven flow of highly viscous liquids that deform in brittle ways as they flow, cool, and slow down.

The Elden Mountain **Pelêan** eruption started three miles north of here with explosions that ejected **pumice, blocks**, and **ash** high above the vent, and ended with extrusion of the lava dome (Fig. 6).

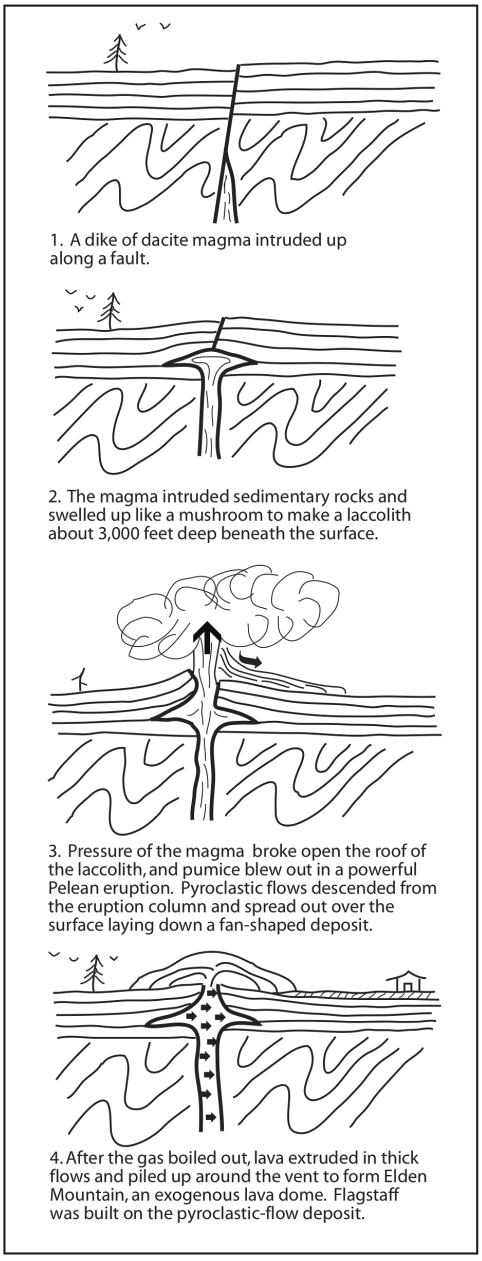

Figure 6. Schematic diagrams illustrating the eruption sequence at Elden Mountain.

The Flagstaff Mall was built on top of the **pyroclastic**-flow deposit, which is also called a block and ash **breccia**. The photograph in Figure 7 shows the breccia preserved in a **paleovalley** eroded in the Kaibab Formation. In the recess marked by the shadow at the bottom of the breccia is a thin pyroclastic surge deposit (Fig. 8).

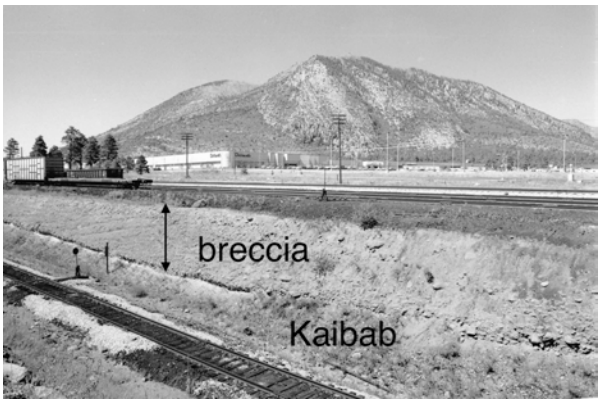

Figure 7. Photograph looking northwest from the Nestle Purina railroad spur, which is private property. Block and ash breccia in exposure, Flagstaff Mall in middle distance, Elden Mountain on skyline.

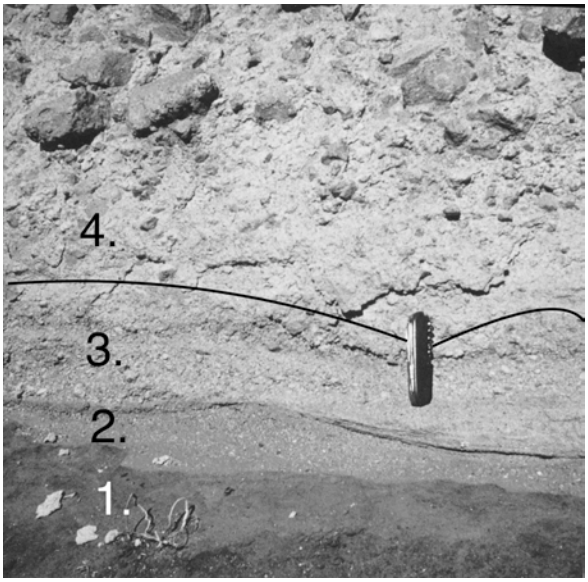

Figure 8. Photograph (1977) of the lower part of the pyroclastic deposits in Figure 7. 1. Thin layer of basaltic ash on Kaibab Formation. 2. Surge bed containing white dacite pyroclasts and basaltic ash eroded from layer 1; low-angle dune form on top of 2 with ash bed below knife on lee side of dune. 3 Surge bed containing sorted dacite lapilli. 4. Block and ash breccia, inversely graded at bottom. Transport was left to right.

Near the Mall the pyroclastic-flow deposit contains isolated blocks of dense and semi-pumiceous dacite enclosed by a matrix rich in ash (Fig. 8); the top of the deposit has been eroded. Elsewhere, the noneroded upper part of the deposit is rich in pumice. Concordant **paleomagnetic** poles of the blocks indicate deposition above about 580º C (K. Tanaka, 1981, oral comm).

A pyroclastic flow is a gravity-driven, ground-hugging, compact system of **fluidized** hot **pyroclasts** and gas that has a high particle concentration, and moves with a quasi-laminar internal flow mechanism. The deposits are coarse, **matrix supported**, structureless, and poorly sorted; inverse grading at the bottom is typical (Fig. 7, 8, 9). A pyroclastic surge is a gravity- and explosion-driven system of pyroclasts and gas that starts out expanded and dilute with a low particle concentration and moves with a turbulent internal flow mechanism; progressive escape of gas causes deflation and increasing particle interaction. The deposits are medium to fine grained, stratified, and sorted, and commonly display current structures such as dunes and cross beds.

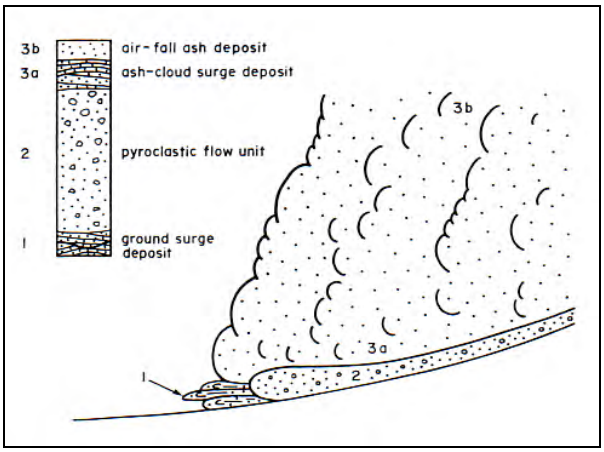

Figure 9. Interpretive sketch showing relations of pyroclastic systems and deposits. Diagram from Cas and Wright, 1987, p. 111.

Exit Mall parking lot and turn right onto US89; middle or left lane.
Continue north on US89 for about 11.6 miles.
Turn right onto FS545 to Sunset Crater Volcano National Monument.
Continue on FS545 for about 1.7 miles; park on paved pull-out on left side of road. Stop 3.

The route to Stop 3 is north along US 89. About two miles north of the Mall, is a large embayment on the east side of Elden Mountain; see on your left and Figure 2. The embayment is on eroded Paleozoic strata that were uplifted when the Elden magma intruded the sedimentary section about 3,000 feet

below the surface and started to form a laccolith (Fig. 6-2); the roof of the laccolith failed, and the eruption began (Fig. 6-3).

The Grand Canyon section from the Permian Kaibab Formation down to the Devonian Temple Butte Formation is exposed here. The Kaibab Formation forms hogbacks about one mile west of the highway (Pk, Fig. 2); dips are 32° to 53° E. At the top of the embayment the Redwall Limestone and Temple Butte Formation dip 28° to 52° E. North of Elden Mountain the gentle north-sloping surface is on the northwest-dipping block of the failed laccolith; dip is 17° NW (Pk, Fig. 2).

Stop 3. Bonito Park. This stop at the east side of Bonito Park is at the base of Bonito terrace. The terrace is significant because excavations here in the early 1930s of pit houses buried by cinders first documented that people were living in this area when Sunset Crater erupted (Colton, 1932).

The view southwest is up the Interior Valley to the Inner Basin of San Francisco Mountain (Fig. 2). The individual peaks on the horseshoe-shaped ridge around the Inner Basin are eroded remnants of stratocones that reached a summit elevation of about 15,400 feet by 0.43 Ma (K/Ar) or 0.51 Ma (Ar/Ar). Humphreys Peak, at 12,633 feet elevation, is the highest in Arizona.

San Francisco Mountain is a compound composite volcano that contains many lava flows, lava domes, and tuff beds from multiple eruptions over a long time (at least 1.42 m.y.). Characteristic features are concave-up slopes, outward dipping lava flows and tuff beds of andesite and dacite, and lava domes of dacite and rhyolite. Core Ridge at the southwest end of the Inner Basin (Fig. 2) is composed of **phaneritic** dikes and plugs that intruded into **agglomerates**, **agglutinates,** breccias, and lavas (Holm 1988, 2021).

Statistics of San Francisco Mountain:

a. Present volume (includes distal lava flows beyond the base): 93 km^3.
b. Volume of Inner Basin, Interior Valley and restored last stratocone: 8 km^3.
c. Original volume: 101 km^3.
d. Volume of debris fans and distal gravel deposits: 9 km^3.
e. Amount removed from volcano: ~8.9 %
f. Estimated percents of **lithologies**:
84% andesite, 14.5% dacite, 1.5% rhyolite.
g. Heights of reconstructed stratocones:
1: 1,700 m, 2: 2,100 m, 3: 2,500 m.
1: 5,576 ft, 2: 6,888 ft, 3: 8,200 ft.
h. Oldest date: 1.82 Ma, rhyolite.
i. Youngest date: 0.40 Ma dacite.

For comparison, a rough volume estimate of the pre-eruption Mount St. Helens is ~35 km^3. The volume removed from the volcano to form the crater is 2.76 km^3 (8 %). The eruption-initiating landslide removed 2.3 km^3 (83.3 % of crater); the subsequent lateral blast removed 0.19 km^3 (6.9 % of crater); the pumice eruption removed 0.27 km^3? (9.8 %? of crater) (Lipman and Mullineaux, 1981).

The Inner Basin originated between 0.43 Ma (K/Ar) or 0.51 Ma (Ar/Ar), the age of the last stratocone, and 0.09 Ma (Ar/Ar), the age of Sugarloaf lava dome that erupted in the mouth of Interior Valley (Fig. 2). Rocks removed from San Francisco Mountain now reside in basal debris fans, the largest of which is on the northeast side (Fig. 2). The large debris fan is key to understanding the origin of Inner Basin.

There are four principal ways that composite volcanoes are degraded to form large valleys (Fig. 10). The Inner Basin is too large and the time available too short for erosion to be the principal factor for its origin; also, the debris fan deposits are not like stream or glacier deposits. A laterally directed explosion followed by a pumice eruption, like Mount St. Helens, or rapid evacuation and collapse of a shallow magma

chamber during a pumice eruption, like Crater Lake, are rejected because complementary deposits rich in pumice have not been found. The time since 430-510 ka seems too short to remove all traces of related pyroclastic deposits.

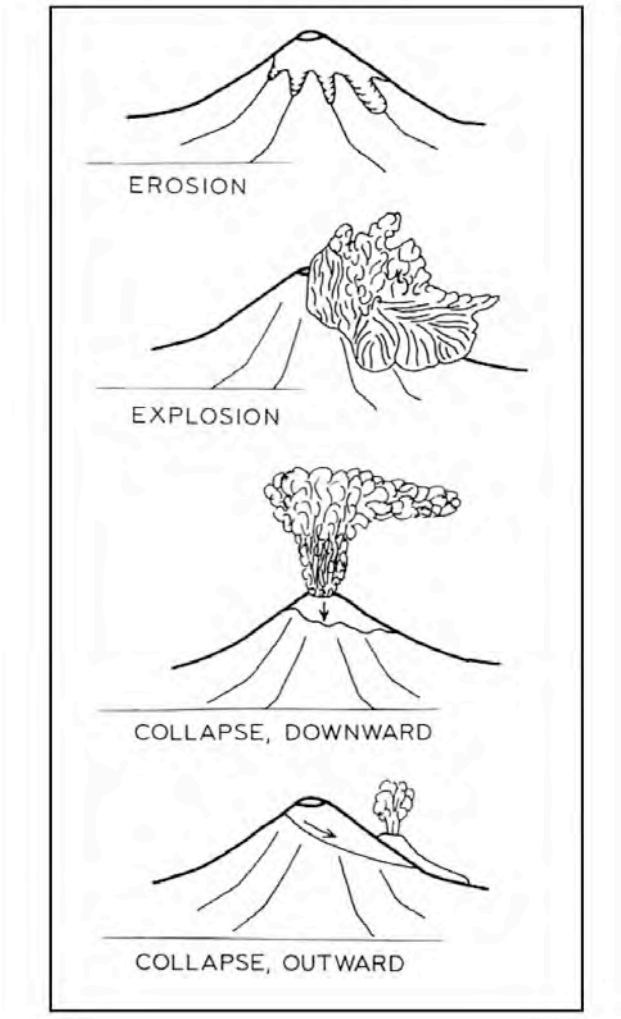

Figure 10. Mechanisms of valley formation on composite volcanoes.

Composite volcanoes are gravitationally unstable because they are high, have steep slopes and weak beds such as tuffs, can be overloaded by summit domes, are inflated by intrusions, and can have hydrothermal alterations. Collapse outward into landslides seems most practical for the origin of Inner Basin.

The debris fan deposits are similar in character to modern landslide deposits from composite volcanoes. They are coarse, poorly sorted, **matrix supported**, lack pumice, and contain blocks of all the rock types that crop out in the Inner Basin. The surface of the largest debris fan is smooth and climbs gradually to an apex at the mouth of the Interior Valley. The debris fan is 375 feet thick in a borehole across the road from Stop 3 (Figs. 2, 13).

Although a large area of the fan has been buried by younger volcanoes and lavas (Fig. 2), all surface and borehole aspects of the debris fan are consistent with an origin by deposition from multiple landslides, such as debris avalanches and debris flows, that originated by gravitational collapse of the northeast sector of San Francisco Mountain.

At its greatest height of 8,200 feet (2,500 m) San Francisco Mountain was poised for collapse. Some of the precursory factors are shown in Figure 11.

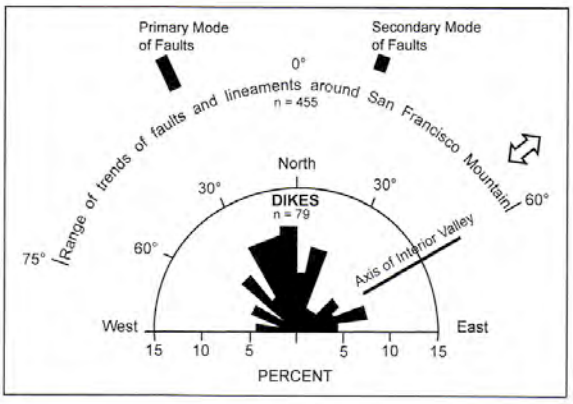

Figure 11. Diagram showing the distribution of orientations of dikes in San Francisco Mountain, the range and modes of fault orientations in the volcanic field, and the orientation of the Interior Valley. The open double arrow shows the direction of tectonic extensional stress in the volcanic field determined from first-motion studies of recent seismicity by Wong and Humphrey (1989). Diagram from Holm (2004).

The basic idea is that northeast directed extensional stress created crustal faults oriented northwest. These faults served as conduits for dikes that intruded up into the volcano in the same orientation. Because the southwest side of the youngest stratocone was buttressed by the older 6,900 ft. (2,100 m) stratocone, dike intrusion inflated the volcano toward the northeast. The summit may have been overloaded by a dacite dome. The idea is illustrated in Figure 12.

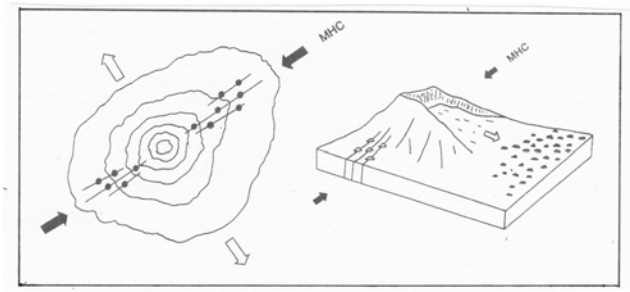

Figure 12. Sketch illustrating the relationships between tectonic stress, dikes, and collapse of a large volcano, from Siebert, 1984. MHC is maximum horizontal compression; open arrows indicate direction of extension.

Some of the evidence for collapse into landslides is in the chip-count data from the borehole, the percentages of which are similar to **lithology** percentages in San Francisco Mountain (Fig. 13, next page). Compare borehole data with Statistics above on p. 7).

In the 110-130 m interval in the lower part of the Layer 3 Volcanic Debris deposit the percentages of andesite (a) and dacite (d) chips cross (Fig. 13, gray shading). Over 80 percent of the dacite chips (**d*** at bottom of Fig. 13) in this interval come from two mapped units in San Francisco Mountain (Holm, 1988; Qddo, Qdhi): a young dome and lava flow on the eastern-most peak (Doyle Peak), and the youngest dike in Core Ridge that fed a **cryptodome** on Humphreys Peak and which could have fed a summit dome; strike of the dike is northwest. High densities of the dacite chips (**d***), which average 2.52 and 2.40, imply the dacite lavas did not generate explosive eruptions of pumice (Holm, 2004).

The abundance of the dacite chips in the 110-130 m interval in the borehole could be evidence for an initial collapse of the northeast sector of San Francisco Mountain.

Possible triggers for gravitational collapse include: tectonic earthquake, volcanogenic earthquake, intense precipitation, or eruption of the 0.40 Ma east-flank dacite lava flow (Figs. 2, 10). Slope failure could also occur spontaneously on a preconditioned volcano.

Unlike Mount St. Helens, a pumice eruption did not follow the landslides at San Francisco Mountain, and no lava extruded in the Inner Basin after it formed. After collapse, the Inner Basin was enlarged by mass wasting, erosion, and glaciation.

Sugarloaf lava dome erupted through the apex of the debris fan 1.5 miles northeast of the Inner Basin (Fig. 2). If Sugarloaf is compared to the Mount St. Helens crater dome it is not in the "crater" but at the base of the composite volcano.

Continue east on FS545 for about 0.25 mile; present Pass or Money at kiosk or if kiosk is not occupied go in Visitor Center.
Continue east on FS545 for about 1.5 miles to entrance to Bonito lava flow parking lot.
Turn right to enter Bonito Flow parking lot.

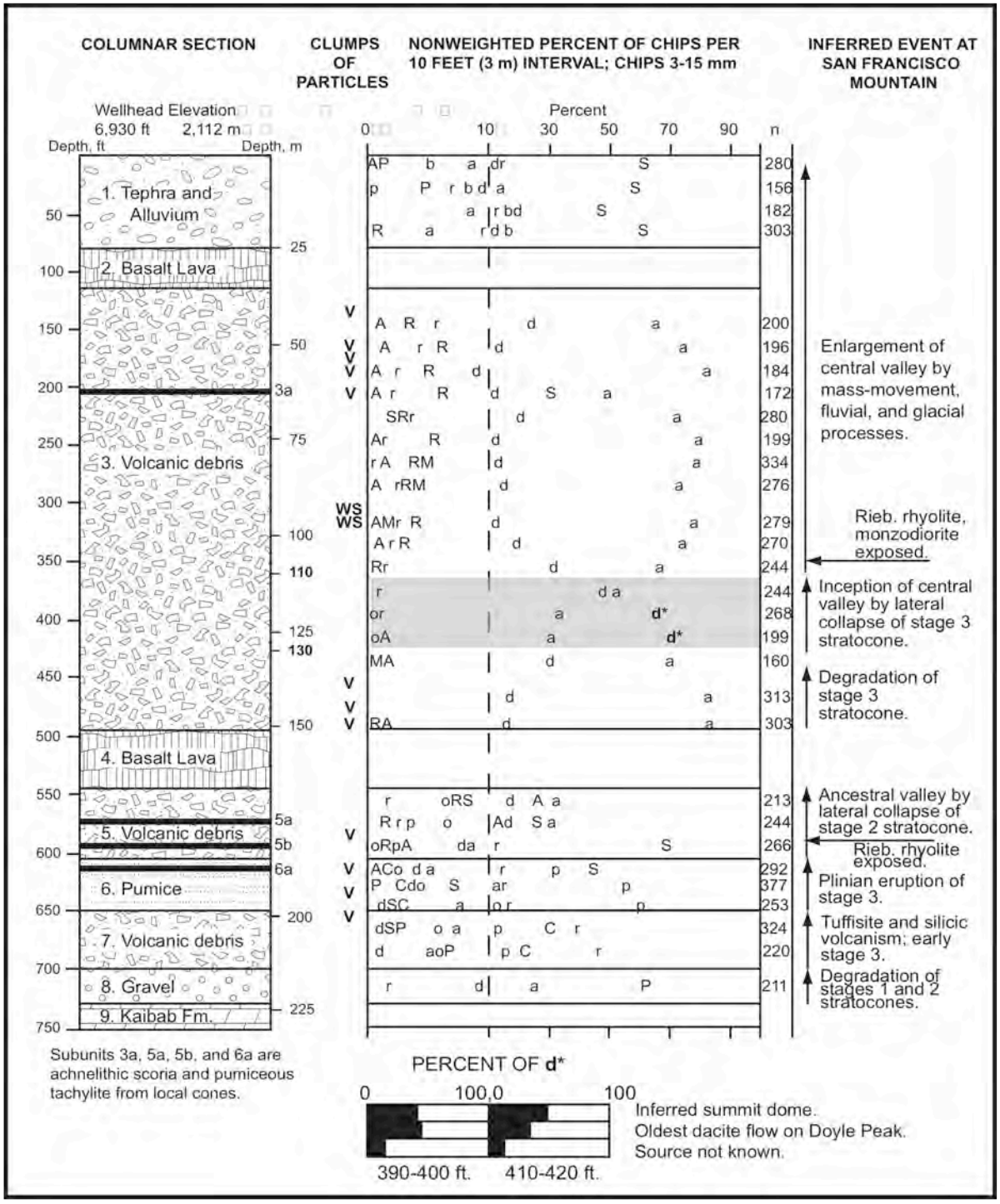

Figure 13. Columnar section constructed from log of borehole shown on Figure 2, and chip-count data of borehole cuttings. Symbols for counted chips of borehole cuttings are: a=andesite, A=hydrothermally altered, b=basalt, C=Precambrian crystalline, d=dacite, M=monzodiorite, o=obsidian, p=pumice, P=Paleozoic limestone and sandstone, r=rhyolite, R=riebeckite rhyolite, S=scoria; n=number of chips counted per sample. Symbols for clumps are: V=contains small vesicles, WS=well sorted. Chips interpreted as hydrothermally altered (A) are earthy, red to orange to yellow, and easily grooved by a teasing needle. Layers 3, 5, and 7 are <u>polymictic</u> deposits that appear to be poorly sorted coarse gravel. Key interval is 110-130 m, shaded gray; see text. Modified from Holm (2004)

Stop 4. Sunset Crater and Bonito Lava Flow. Sunset Crater is the youngest volcano in the San Francisco volcanic field (Figs. 2 and 14). The cinder cone is about 290 m (960 ft) high and 1630 m (5350 ft) in basal diameter; the summit crater is about 140 m (460 ft) deep. The prevailing southwest wind during the eruption built the crater rim higher on the northeast side.

Powerful **Strombolian** to **subPlinian** eruption columns might have reached more than 20 km (12.4 mi) above the vent (Alfano et al., 2019). Cinders fell beyond the Wupatki area 13 miles to the northeast (Fig. 2, Stop 5). After the eruption, Wupatki Pueblo was constructed on top of the cinder blanket.

The red cinders at the top of the cone were colored by oxidation of ferrous iron in the black glassy cinders to form hematite, either by escaping volcanic gas after the cone was constructed (most likely), or by steam from precipitation that fell on hot cinders. The summit cinders are cemented by hematite, gypsum, opaline silica, and sulfur (Hanson, 2003).

The last summit eruption produced the small crater on the east side of the summit (Fig. 15) and ejected black **lapilli** and **bombs**, some of which fell beyond the base of the cone as far as three-quarters of a mile from the vent.

Sunset Crater is at the northwest end of a six-mile-long row of vent structures that are probably fault controlled (Fig. 2). The eruptive event began at vent 512, shifted northwest to Gyp Crater and two rows of small cones, and ended at Sunset Crater.

No direct dates have been obtained on the eruption products. Indirect dates from multiple studies by different methods suggest the eruption occurred sometime during the second half of the 11th century. The first **dendrochronological** analysis of beams in Wupatki Pueblo (Stop 5) proposed that they came from trees that survived the eruption and were harvested later to build the pueblo. Aberrant growth rings, not found in timbers outside the cinder blanket, suggest that the eruption began between the growing seasons of A.D. 1064 and 1065 (Smiley, 1958).

Paleomagnetic data plotted on the southwest archaeomagnetic master curve allow for an eruption between A.D.1030 and 1170, but narrowed to A.D. 1040 to 1100 with geological considerations (Ort et al., 2002). Ceramic assemblages and dendrochronology place the eruption between A.D. 1046 and 1080 (Downum, 1988). Dendrochronology and dendrochemistry of beams from nearby archaeological sites point to an eruption date about A.D. 1085 (Alfano et al., 2019).

Sunset Crater erupted with two cone-building stages. The first stage ended with deposition of an agglutinate carapace around the summit, and the second stage erupted cinders that built the modern symmetrical cone. Extrusion of Stage 1 of the Bonito lava flow breached the first cone, which caused the agglutinate layers to collapse onto the emerging lava. The mounds of agglutinate were carried northwest as the flow advanced (Figs. 14, 15). Continued, or renewed, eruption of cinders restored Sunset Crater to its present symmetrical shape before extrusion of Stage 3 of Bonito lava flow.

Figure 14. View of the northwest side of Sunset Crater, and an agglutinate mound in the foreground on Stage 1 of the Bonito lava flow. The mound is ~120 feet (37 m) high; rootless lava flows on the mound dip 10° west (right).

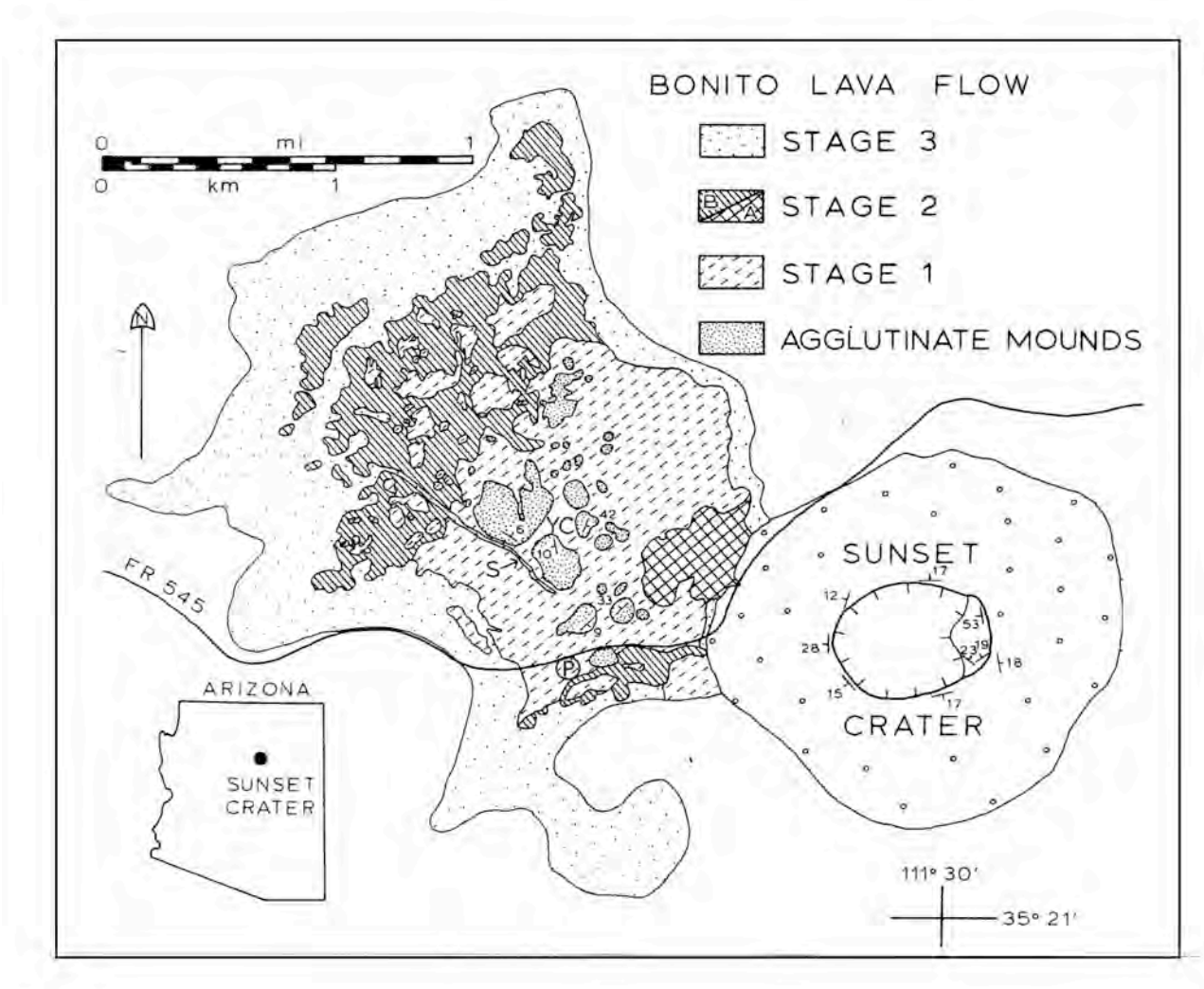

Figure 15. Map of Sunset Crater and Bonito lava flow. The Bonito lava flowed into an intercone basin, which controlled the shape of the lava's periphery; can you see "Madam Bonito"? The lava may be as much as 100 feet thick in the center (Hanson, 2003). Strike and dip symbols show orientation of bedding in cemented cinders on the rim of Sunset Crater, and orientation of layers in agglutinate mounds that collapsed onto the emerging Stage 1 of the Bonito flow as it breached the west side of an early-stage cone of Sunset Crater. The breached cone was restored to the present symmetry by continued eruption of cinders. P is parking lot. YC is Colton's (1937) Yaponcha Crater; S is longest squeeze-up. Modified from Holm, 1987.

Characters of Bonito lava flow stages:

Stage 1: High level. Continuous cinder cover ~1 m thick. Numerous thin **flow units**.

Stage 2A: Extruded onto Stage 1 from a spatter rampart that was fed by a northwest-striking dike at the base of Sunset Crater. Continuous cinder cover, but cinder blanket is only a few centimeters thick.

Stage 2B: Extruded from lava tubes in Satge 1. Various **pahoehoe** types, but mostly slab pahoehoe. Thin and patchy cinder cover that thickens with larger cinders toward Sunset Crater.

Stage 3: Extruded from many lava tubes around the periphery of Stages 1 and 2. Low level. Mostly **aa**, but some slab pahoehoe. No cinder cover; some cinders in cracks.

Self-guiding Trail Guide

Follow the Lava Flow Trail at the east end of parking lot to observe features of the Bonito basalt lava flow (SiO_2=46.90-47.38). You are in a National Monument. Please stay on the trail and do not disturb rocks or plants.

1. Paved trail on Stage 1. Cinder cover ~1 m thick is typical of Stage 1. Red agglutinate mound on left.
2. Before bridge: Stage 2B **pahoehoe** flow unit that broke out of a lava tube and covered Stage 1.
3. Bridge crosses collapsed **lava tube** of Stage 2B.
4. Far end of bridge: look back on left to see lava blister (crust puffed up by gas) with lavacicles on roof; look right to see white Kaibab Formation **xenoliths**.
5. Trail on "island" of Stage 1; thick cinder cover.
6. Turn right at fork in trail. Go 175 yards to platform.
7. Squeeze-up. Formed when Stage 3 lava pushed partly solidified Stage 2B lava out of lava tube. Stage 3 lava extruded from end of tube and formed the clinker-covered **aa** lava flow at the lower level that lacks a cinder cover (see down to your left).
8. Turn around and continue north on paved trail to sharp left bend. Make a decision: stay on paved trail back to parking lot, or, turn right on narrow cinder trail.
9. Cinder trail: On Stage 2B lava; thin (cm) cinder cover; lava is mostly slab pahoehoe, but massive, ropy, and festoon pahoehoe and pahoehoe toes can be found (But Stay On Trail).
10. Small open area crosses Stage 1 lava (thicker cinder cover) surrounded by pahoehoe of Stage 2B.
11. Cinder cover on Stage 2B thickens and coarsens toward Sunset Crater. Continue past "12" post.
12. Hornito: ("little oven") a rootless spatter cone, 20 feet high on left, made of agglutinated bombs ejected through a crack in the crust of Stage 2B from an underlying lava tube. Weak explosions drive ejection heights and ballistic ranges that are just a few feet.
13. "10 post". Entrance to partly evacuated and collapsed lava tube. CLOSED-stay out.
14. Along trail is row of four hornitos that erupted on the crust of Stage 2B from underlying lava tube; row projects back to Sunset Crater.
Trail bends right at 4th hornito (open circular rampart).
15. Trail climbs up on lower edge of Stage 1 lava pushed up by inflation of subjacent Stage 2B lava; red cinders suggest either that Stage 1 lava was still hot when cinders landed, or oxidation was by gas escaping from underlying Stage 2B lava.
16. Trail descends to Stage 3 lava flow at a lower level; flow is slab pahoehoe and aa lava. No cinder cover. (Wind blew fine cinders along the edge onto the lava).
17. Fork in trail: continue straight along fence.
18. Concrete bench: end of squeeze-up; one of the extrusion points of Stage 3 lava.
19. Steps: climb up steep edge of Stage 2B lava flow.
20. Return to parking lot on paved trail.

Return to FS545; turn right, continue east for about 17.5 miles. Route to Stop 5 presents views of Little Colorado River valley and Painted Desert. Turn left into parking lot for Wupatki Visitor Center. Stop 5.

Stop 5. Wupatki Pueblo and Blowhole. In the parking lot, seen counterclockwise from east to west (Fig. 2): 0.15 Ma basalt; Triassic strata in Painted Desert; Little Colorado River; Black Point monocline and basalt flow (0.87 Ma); Doney fault; Doney cinder cones at Stop 6; Woodhouse Mesa basalt (0.96 Ma).

Wupatki Pueblo was built and occupied in the 12th century, and was abandoned in the 13th century. Buy a trail guide for the pueblo in the Visitor Center.

The blowhole at the far end of the paved trail is one of numerous entrances to solution-formed open fissures and caverns in the Kaibab Formation, which is about 300 feet thick in this area. A gravity survey of an area containing several blowholes indicated the absence of large caverns; the largest cavern might be 50 ft. wide (Lamar, 1964).

Multiple branched, and interconnected passages are thought to link the blowholes. Zinc-cadmium-sulfide powder introduced into a blowhole during an intake cycle was subsequently detected at other blowholes up to 24 miles distant (Sartor, 1964). Volume of the open system in the Wupatki area is estimated to be at least $7x10^9$ ft^3 (Sartor, 1964). Some open fissures, locally called "earth cracks" in the Wupatki area, have been explored as deep as 500 ft (Lamar, 1964).

During diurnal cycles, air flows in during the night and early morning under higher barometric pressure and cooler air temperatures, and flows out during the late morning and afternoon under lower barometric pressure and warmer air

temperatures. Average intake velocities are 6-7 mph, and average exit velocity is about 22 mph; exit velocities up to 30 mph have been recorded (Schley, 1961). The air flow also responds to barometric pressure changes associated with thunder storms.

Return to FS545; turn left, continue on FS545 for about 4.2 miles. Turn left into Doney Picnic Area. Stop 6.

In gully on the right see the Triassic-Permian contact (red Moenkopi Formation on light gray to tan Kaibab Formation). Views of the Black Point **monocline** and Doney fault structural system are ahead. The road passes between a **fault-line scarp** on the right and Doney Mountain cinder cone on the left (Fig. 2); on the left see planar-bedded cinder deposits in the cone that contain white carbonate xenoliths. Reddish-orange **palagonite** in the lower part of the cinders indicates initial hydromagmatic eruption involving ground water.

Stop 6. Doney Picnic Area. Doney Mountain is the prominent cinder cone northeast of the picnic area. The Doney cinder cone and an associated row of three small coalesced cones to the south erupted along the Black Point monocline-Doney fault structural system (Figs. 2, 16). The monocline and fault formed by compression forces during the Laramide **orogeny** 75-45 million years ago.

An optically stimulated luminescence date (OSL) suggests the Doney eruption occurred about 68-70 thousand years ago (Billingsley et al., 2007).

The cinder trail on the south side of the parking lot starts on eroded Kaibab Formation limestone, crosses black cinders from Sunset Crater, passes by a vent-proximal agglutinate deposit of welded bombs, and climbs three cinder cones on red pyroclasts that increase in size near the summit vents. Some **fusiform bombs** are longer than one

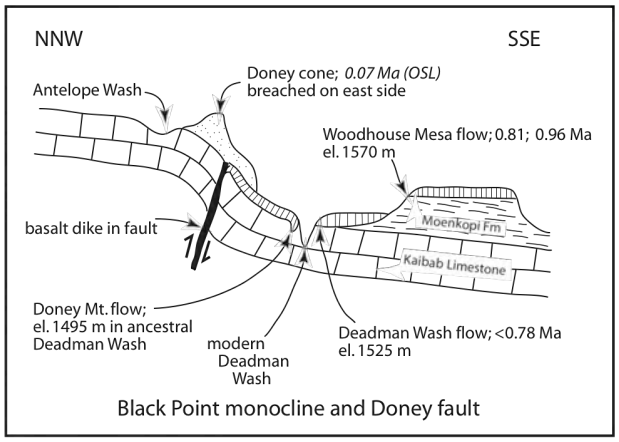

Figure 16. Cross section sketch showing relations of tectonic structures, erosion surfaces, and lava flows in the Doney Mountain area.

meter. Elevation gain is 215 feet to the top of the southern cone.

These cinder deposits are typical of Strombolian eruptions, which are characterized by pulsating gas explosions in near-surface basalt magma. When the magma is degassed, a lava flow commonly extrudes.

The summit of the southern cone is crescent shaped, not circular, because the rising lava breached the east side of the cone opposite the monocline (Fig. 16), which caused the cinders to collapse onto the emerging lava flow. Lava typically pushes out from the base of a cinder cone rather than extruding from the summit vent because the lava is denser than the cinder cone, and unconsolidated cinders commonly lack the strength to support a column of lava.

Some of the structural and geomorphic features seen clockwise from the summit of the southern cone include:

(1) Painted Desert (east).
(2) East-dipping Kaibab Formation (~13°) on the Black Point monocline (south).
(3) San Francisco Mountain (southwest).
(4) S P Crater (west; Stop 8).
(5) Gray Mountain-East Kaibab monocline (northwest).
(6) terminus of Citadel lava flow (north).
(7) Black Point lava flow (north).

(8) Basalt lava flows seen to the east from oldest to youngest, and highest to lowest, are: Woodhouse Mesa flow; Deadman Wash flow; and three flows from the Doney cinder cones (SiO_2=48.18-49.02) (Figs. 2, 16, 17).

All of these lava flows followed tributary paleovalleys and slopes toward the Little Colorado River on successively lower and younger erosion surfaces (Cooley, 1962). Modern Deadman Wash is incised below the youngest lava flow (Figs. 16, 17, Doney Mountain flow).

Antelope Wash is the abandoned drainage along the west side of the row of cones (Fig. 16). After Deadman Wash had captured Antelope Wash, the Deadman Wash lava flow entered and flowed down the lower and younger Deadman Wash (Holm, 2001b).

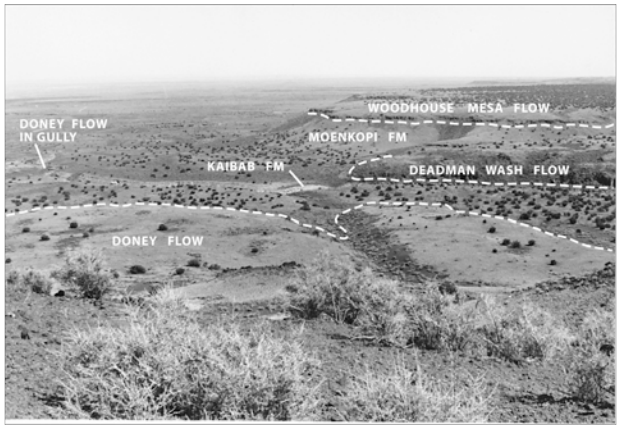

Figure 17. Photograph of lava flows and erosion surfaces seen east of southern Doney cinder cone. Modern Deadman Wash is incised in Kaibab Fm.

Return to FS545; turn left, continue on FS545 for about 5.2 miles. Turn left into Citadel Pueblo parking lot. Stop 7.

The road to Stop 7 first crosses the abandoned Antelope Wash, then is on the erosion-stripped surface of the Kaibab Formation. Most of the Moenkopi Formation has been eroded off the top of the Black Point monocline except where it is protected by basalt lava flows.

Stop 7. Citadel Pueblo. Walk on trail to Citadel Pueblo. Citadel Pueblo is a Sinagua Indian structure that was constructed on top of a basalt lava flow. The Citadel lava flow and the Black Point lava flow to the north (Fig. 2) have the same petrography (plagioclase **phenocrysts** 1-2 cm) and field position on the monocline, and practically the same Ar-Ar ages (Fig. 2, ~0.87 Ma; Hanson, 2010), which suggest they came from the same vent or related vents. Both lavas flowed northeast down tributary valleys of the Little Colorado River. The Black Point flow reached the river and filled the channel, forming Black Point (Fig. 2).

The K-Ar age of the Black Point lava flow is 2.43 Ma, which is considerably older than the Ar-Ar age (Fig. 2). The calculated rate of incision of the Little Colorado River at Black Point using the Ar-Ar date is ~250 m/m.y. This rate is closer to the incision rate of the Colorado River below Lees Ferry (~170-230 m/m.y., Darling et al., 2012) than the rate calculated with the K-Ar date (~90 m/m.y., Damon et al., 1974).

Exposed on the south side of Citadel sink is a paleovalley that was eroded in the Moenkopi Formation and subsequently filled by the Citadel lava flow (Fig. 18). The paleovalley was a tributary to the now abandoned Antelope Wash.

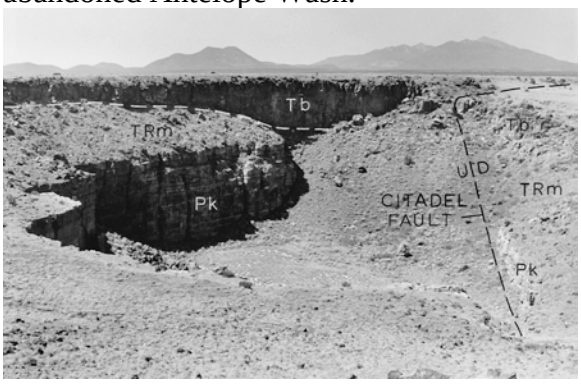

Figure 18. Photograph looking south across Citadel sink toward O'Leary Peak (left) and San Francisco Mountain (right). Citadel lava flow (Tb) thickens in a paleovalley eroded in Moenkopi Formation (TRm). Kaibab Formation is (Pk). Citadel fault moved down (D) on its northwest side.

The Citadel lava flow now forms a dark ridge that extends about 4.3 miles northeast of the pueblo (Fig. 2). Where the Moenkopi Formation was not protected by the lava flow it was eroded off of the Kaibab Formation and the topography was inverted (Fig. 19).

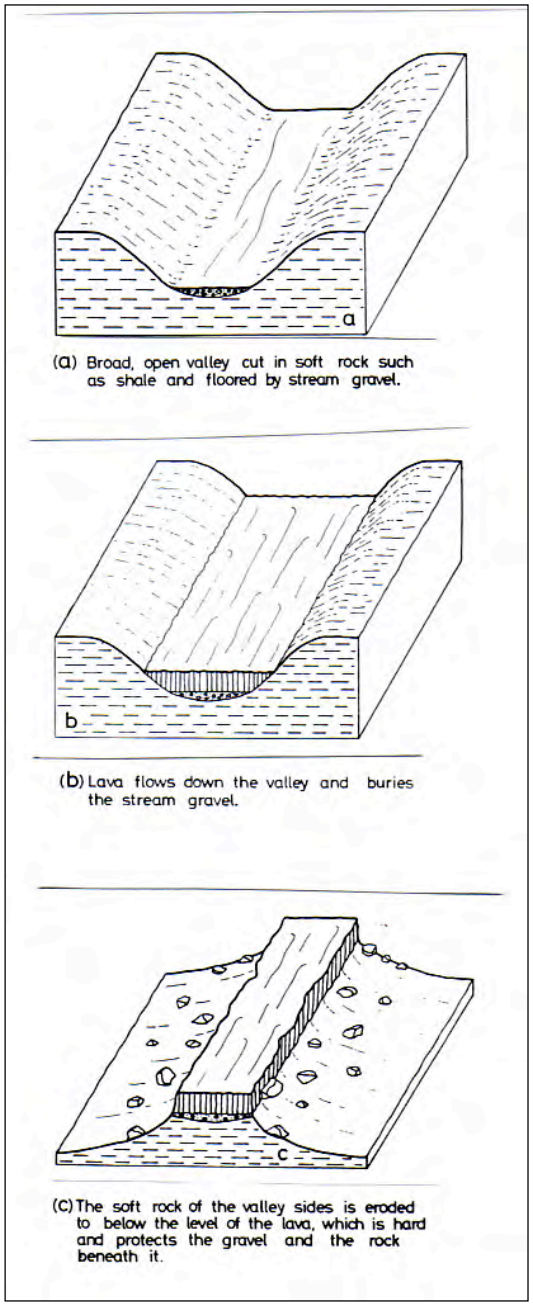

Figure 19. Diagrams illustrating the process of inversion of topography (from Lucchitta, 1984). A low-lying valley becomes a high-standing ridge.

The southeast bounding fault of the Citadel graben displaces the Kaibab Formation by about 16.5 m (54 ft), of which about 6.5 m (21 ft) postdates the Citadel lava flow (Fig. 18). Solution of the limestone along the fault by ground water caused the sink to form by collapse, possibly during wet periods in the Pleistocene Epoch.

Return to FS545 and turn left. Continue on FS545 for about 4.1 miles to US89.

FS545 to US89 crosses the Citadel graben, then the Cedar Canyon graben, and then the Black Point lava flow.

Turn right onto US89. Continue north on US89 for about 3.0 miles (about 1.7 miles past Hank's Trading Post). Turn left onto graded road: **BE ALERT FOR ONCOMING & REAR TRAFFIC.** *Continue on graded road for about 7.3 miles; park on right side of road just beyond left lava levee. Stop 8.*

West of US89, the gravel road to Stop 8 crosses several basalt lava flows that are about one million years old (Fig. 2). The black hummocks on the surface are tumuli, small dome-like structures where the flow's crust was pushed up by internal fluid pressure of the lava. **Block lava flow** with steep sides on the right is from S P Mountain (Fig. 2). Stop 8 is at base of S P Mountain.

Stop 8. S P Mountain. S P Mountain (or S P Crater) is a cinder cone 250 m (820 ft) high and 1200 m (3900 ft) in basal diameter; its summit crater is 400 m (1300 ft) across and about 120 m (400 ft) deep (Fig. 20). Welded spatter, large bombs (1-4 m), and **rootless flows** (SiO_2=54.78) form an agglutinate collar around the crater's rim (Ulrich, 1987). The slopes are mantled by bombs and lapilli.

Figure 20. Oblique aerial photograph of S P Mountain cinder cone and lava flow. View is north-northeast. Photograph U.S. Geological Survey.

A high precision K-Ar date of the associated lava flow is 71 +/- 4 **ka** (Baksi, 1974, revised for new decay constants); polarity is normal. More recently, different dating methods have returned dates of: 72 ka (Ar/Ar), 43-82 ka (He-3, Ne-21), 6 ka (OSL), 60 ka (He-3) (Rittenour et al., 2015).

The blocky basaltic andesite lava flow (SiO_2=56.80) extruded early in the eruption and flowed north down a graben for 7 km (4.3 mi) (Figs. 2, 21). The graben and its interior **horst** directed the course of the lava. The lava flow is 15 m (50 ft) thick at its proximal end, and is 55 m (180 ft) thick at its terminus.

The flow extruded concurrently with Strombolian explosions at the vent; large bombs that lie on top of the flow far beyond ballistic range must have been carried away by the flow.

The ridges along the flow's margins near the cone are **lava levees** that formed when the center of the flow drained forward at the end of the effusion stage and left the solidified sides standing higher. Because the base of the cone is not disturbed and overlies the lava flow, the last stage of cone building is interpreted to postdate the flow.

The lower flank of the cone on its north side is partly overlain by **protalus ramparts** of coarse debris that probably slides down on winter snow banks (Bill Breed, personal comm.).

The basaltic andesite lava flow contains phenocrysts of olivine, clinopyroxene, embayed and sieved plagioclase, embayed quartz, and sparse hypersthene in a **hypocrystallline** groundmass (Ulrich 1987).

East of S P Mountain is a row of cinder cones that erupted along the projection of the east bounding fault of the graben (Figs. 20, 21). Several of the cones are elongated along the trace of the fault.

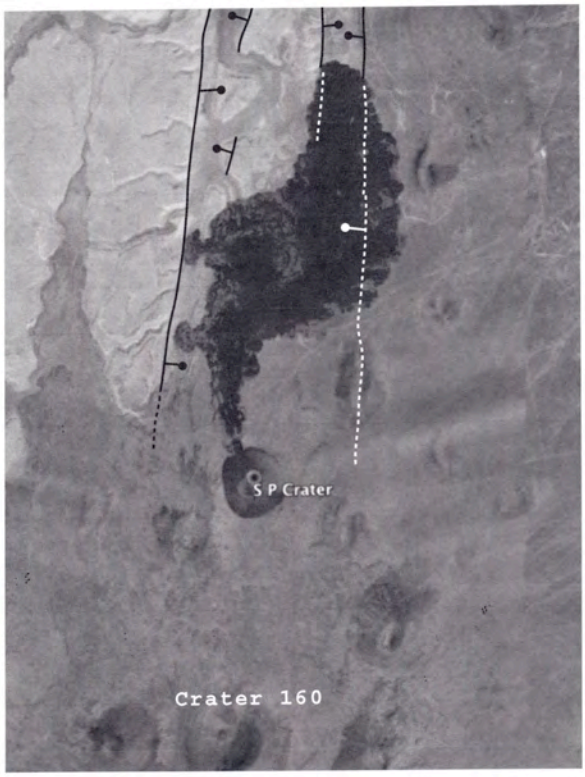

Figure 21. Google Earth image of S P Crater and its associated block lava flow. "Cleft" cinder cones are lined up along the trace of the east-bounding fault of the graben. Kaibab Formation is light tone in upper left corner. Gray tone is cinder blanket and cinder cones. Ancient stream channel meanders in graben. Faults taken from Ulrich and Bailey, 1987.

During Spring months restrictions might be imposed on the SP Crater Golden Eagle Conservation Complex. For information contact Babbitt Ranches in Flagstaff 928-774-6199 or Arizona Game and Fish Department in Flagstaff 928-774-5045.

Drive 0.05 mile west to turn around on left at entrance to dirt track.
Return to US89, turn right. Return to Flagstaff.

The route on US89 from the last stop (Stop 8) back to Flagstaff climbs up along the top of the debris fan (Fig. 2); note the even grade and large boulders on the fan surface.

On entering Flagstaff continue on US89/Santa Fe Avenue/Route 66 to downtown Flagstaff.

REFERENCES CITED

Alfano, F., Ort, M., Pioli, L., Self, S., Hanson, S., Roggensack, K., Allison, C., Amos, R., and Clarke, A., 2019, Subplinian monogenetic basaltic eruption of Sunset Crater, Arizona, USA: Geological Society of America Bulletin, v. 131, no. 3-4, p. 661-674.

Baksi, A.K., 1974, K-Ar study of the S.P. flow: Canadian Journal of Earth Science, v. 11, p. 1350-1356.

Ben-Horin, J.y., Pearthree, P.A., Holm, R.F., and Heizler, M., 2021, Detailed geologic and geomorphic mapping and characterization of the Lake Mary fault zone, Coconino County AZ: Arizona Geological Survey Open-File Report OFR-21-02, 16 p.

Billingsley, G.H., Priest, S.S., and Felger, T.J., 2007, Geologic map of Wupatki National Monument and vicinity, Coconino County, northern Arizona, U.S. Geological Survey Scientific Investigations Map 2958, 1:100,000.

Cas, R.A.F. and Wright, J.V., 1987, Volcanic successions modern and ancient: London, Allen & Unwin, 528 p.

Colton, H.S., 1932, Sunset Crater. The effect of a volcanic eruption on an ancient pueblo people: Geographical Review, v. 22, p. 582-590.

Colton, H.S., 1937, The basaltic cinder cones and lava flows of the San Francisco Mountain volcanic field, Arizona: Museum of Northern Arizona Bulletin 10, 49 p.

Conway, F.M., Ferrill, D.A., Hall, C.M., Morris, A.P., Stamatakos, J.A., Connor, C.B., Halliday, A.N., and C. Condit, 1997, Timing of basaltic volcanism along the Mesa Butte Fault in the San Francisco Volcanic Field, Arizona, from $^{40}Ar/^{39}Ar$ dates: Implications for longevity of cinder cone alignments: Journal of Geophysical Research, v. 102, no. B1, p. 815-824.

Cooley, M.E., 1962, Geomorphology and the age of volcanic rocks in northeastern Arizona: Tucson, Arizona Geological Society Digest, v. V., p. 97-115.

Crow, R., Karlstrom, K., Asmerom, Y., Schmandt, B., Polyak, V ., and DuFrane, S.A., 2011, Shrinking of the Colorado Plateau via lithospheric mantle erosion: Evidence from Nd and Sr isotopes and geochronology of Neogene basalts: Geology, v. 39, no. 1, p. 27- 30.

Damon, P.E., Shafiqullah, M., and Leventhal, J.S., 1974, K-Ar chronology for the San Francisco volcanic field and rate of erosion of the Little Colorado River, *in* Karlstrom, T.N.V., et al., eds., Geology of northern Arizona: Flagstaff, Arizona, Geological Society of America Rocky Mountain Section Guidebook, p. 221–235.

Darling, A.L., Karlstrom, K.E., Granger, D.E., Aslan, A., Kirby, E., Ouimet, W.B., Lazear, G.D., Coblentz, D.D., and Cole, R.D., 2012, New incision rates along the Colorado River system based on cosmogenic burial dating of terraces: Implication for regional controls on Quaternary incision: Geosphere, v. 8, no. 5, p. 1020-1041.

Downum, C.E., 1988, "One Grand History": A critical review of Flagstaff archaeology, 1851-1988 [Ph.D. dissertation]: Tucson, University of Arizona, 530 p.

Hanson, S.L., 2003, Roadside Geology: Wupatki and Sunset Crater Volcano National Monuments: Arizona Geological Survey, Down-To-Earth Number 15, 36 p.

Hanson, S.L., 2010, Geochemistry and age determinations of lava flows in the northeastern San Francisco volcanic field, northern Arizona: Cordilleran Section-106th Annual Meeting, and Pacific Section, American Association of Petroleum Geologists, paper no. 44-4.

Holm, R.F., 1987, Significance of agglutinate mounds on lava flows associated with monogenetic cones: An example at Sunset Crater, northern Arizona: Geological Society of America Bulletin, v. 99, p. 319-324.

Holm, R.F., 1988, Geologic map of San Francisco Mountain, Elden Mountain, and Dry Lake Hills, Coconino County, Arizona: U. S. Geological Survey Miscellaneous Investigations Series Map I-1663, 1:24,000.

Holm, R.F., 2001a, Cenozoic paleogeography of the central Mogollon Rim-southern Colorado Plateau region, Arizona, revealed by Tertiary gravel deposits, Oligocene to Pleistocene lava flows, and incised streams: Geological Society of America Bulletin, v. 113, no. 11, p. 1467-1485.

Holm, R.F., 2001b, Pliocene-Pleistocene incision on the Mogollon Slope, northern Arizona: Response to the developing Grand Canyon: *in* Young, R.A., and Spamer, E.E., eds., The Colorado River: Origin and evolution: Grand Canyon, Arizona, Grand Canyon Association Monograph 12, ch 8, p. 59-63.

Holm, R.F., 2004, Landslide preconditions and collapse of the San Francisco Mountain composite volcano, Arizona, into cold debris avalanches in late Pleistocene: The Journal of Geology, v. 112, p. 335-348.

Holm, R.F., 2021, Petrography, geochemistry, and volcanogenic development of the San Francisco Mountain volcanic system, northern Arizona: Arizona Geological Survey CR-21-C, 36 p., 5 appendices.

Karatson, D., Telbisz, T., and Singer, B.S., 2010, Late-stage volcano geomorphic evolution of the Pleistocene San Francisco Mountain, Arizona (USA), based on high-resolution DEM analysis and $^{40}Ar/^{39}Ar$ chronology: Bulletin of Volcanology, v. 72, p. 833-846.

Lamar, D.L., 1964, Geology of the Wupatki blowhole system: Plateau, v. 37, no. 1, p. 35-40.

Lipman, P.W., and Mullineaux, D.R., 1981, The 1980 eruptions of Mount St. Helens, Washington: U.S. Geological Survey Professional Paper 1250, 844 p.

Lucchitta, Ivo, 1984, Development of landscape in northwest Arizona: The country of plateaus and canyons, *in* Smiley, T.L., et al., eds., Landscapes of Arizona: Lanham, Maryland, University Press of America, p. 269 –301.

McKee, E.H., Damon, P.E., Shafiquallah, M., Harris, R.C., and Spencer, J.E., 1998, Compilation of unpublished USGS and University of Arizona K-Ar dates of volcanic rocks of the San Francisco volcanic field, northern Arizona: Arizona Geological Survey Open-File Report 98-2, 25 p.

Morgan, P., Sass, J.H., Duffield, W., 2010, Geothermal resources evaluation program of the eastern San Francisco volcanic field, Arizona: Arizona Geological Survey, Contributed Report CR-10-D, 69 p.

Ort, M.H., Elson, M.D., Champion, D.E., 2002, A paleomagnetic dating study of Sunset Crater volcano: Technical Report No. 2002-16, Desert Archaeology, Inc., 16 p.

Reynolds, S.J., Florence, F.P., Welty, J.W., Roddy, M.S., Currier, D.A., Anderson, A.V., and Keith, S.B., 1986, Compilation of radiometric age determinations in Arizona: Arizona Bureau of Geology and Mineral Technology Geological Survey Branch Bulletin 197, 258 p.

Rittenour, T., et al., 2015, How old are the SP and Strawberry volcanic vents and flows in the San Francisco volcanic field? New evidence from soils, OSL dated loess and He-3 exposure dating: Geological Society of America Annual Meeting, paper no. 312-6.

Sartor, J.D., 1964, Meteorological investigation of the Wupatki blowhole system: Plateau, v. 37, no. 1, p. 26-34.

Schley, R.A., 1961, Diurnal air flow through an Earth crevice, Wupatki National Monument: Plateau, v. 33, no. 4, p. 105-111.

Siebert, L., 1984, Large volcanic debris avalanches: characteristics of source areas, deposits, and associated eruptions: Journal of Volcanology and Geothermal Research, v. 22, p.163–197.

Smiley T.L., 1958, The geology and dating of Sunset Crater, Flagstaff, Arizona: New Mexico Geological Society Field Conference Guidebook 9, p. 186-190.

Ulrich, G.E., Billingsley, G.H., Hereford, R., Wolfe, E.W., Nealey, L.D., and Sutton, R.L., 1984, Map showing geology, structure, and uranium deposits of the Flagstaff 1° x 2° quadrangle, Arizona: U.S. Geological Survey Miscellaneous Investigations Map I-1446, scale 1:250,000, 2 sheets.

Ulrich, G.E., 1987, SP Mountain cinder cone and lava flow, northern Arizona: Geological Society of America Centennial Field Guide-Rocky Mountain Section, p. 385-388.

Ulrich, G.E., and Bailey, N.G., 1987, Geologic map of the SP Mountain part of the San Francisco volcanic field, north-central Arizona: U.S. Geological Survey Miscellaneous Field Studies Map MF-1956, 1:50,000.

Wong, I. G., and Humphrey, J. 1989, Contemporary seismicity, faulting, and the state of stress in the Colorado Plateau; Geological Society of America Bulletin: v. 101, p.1127–11

GLOSSARY

aa the type of basalt lava consisting of, or mantled by, rough fragments, called clinkers that are covered by spiny protrusions.

achnelithic scoria glassy cinders that have smooth rounded surfaces; typically elongated.

agglomerate a deposit of volcanic bombs and coarse lapilli that is weakly to strongly consolidated by compaction or cementation.

agglutinate a deposit of volcanic bombs and coarse lapilli that is strongly consolidated by fusion, or welding together, of the pyroclasts while they are still hot and incandescent.

ash pyroclasts smaller than 2 mm.

block a general term for a large angular rock fragment. Volcanic blocks are larger than 64 mm; they can originate by explosions or flow of viscous lava.

block lava flow the type of lava flow consisting of, or mantled by, blocks. Typically andesite and dacite.

bomb a rounded volcanic fragment (pyroclast) larger than 64 mm; ejected from a volcano in a molten state. Surface tension of the lava during flight shapes the surface.

breccia a general term for weakly to strongly consolidated rocks composed of large angular fragments; the fragments may be embedded in a finer-grained matrix. Breccias can originate by volcanic, sedimentary, tectonic, and geomorphic processes.

colluvium unconsolidated soil and rock debris moved slowly down slopes by gravity.

columnar joints tension fractures in lava flows that form perpendicular to the cooling surface. Typically steep to vertical in lava flows and horizontal in vertical dikes.

cryptodome a "hidden dome". A dome intruded into a volcano, typically a composite volcano.

cuesta an asymmetrical ridge on a tilted layer of rock that is resistant to erosion; the gentler slope is in the direction of tilt (or dip). Typically paired with a weak, easily eroded layer.

dendrochronology the technique of dating the age of a tree by counting its tree rings.

dip slope a land surface that slopes parallel with the dip (or tilt) of the underlying layer of strata.

fault-line scarp an escarpment along a fault that was uncovered by erosion of overlying rocks. A **fault scarp** is the original break of the land surface due to fault movement.

flow unit a single layer of lava in a field of lava flows.

fluidized the state of a gas-fragment system where the gas pressure and flow rate are sufficient to separate the solid fragments and keep them apart. The effect is minimal internal friction and high mobility of the system.

fusiform bomb a bomb with a rounded, elongated shape like a spindle. The shape forms by surface tension during the flight time of a molten clot of lava ejected from a volcano. The shape is not due to spiraling in the air like a football.

graben a block of rock that has moved down along faults on two sides under extensional force. The surface expression is a valley bound on both sides by fault scarps.

holocrystalline the texture of a rock that is composed entirely of crystals; no glass.

horst a relatively higher block of rock separated from lower ground on two sides by parallel faults. Commonly associated with grabens in areas of extensional stress.

hypocrystalline the texture of a rock that contains crystals in a matrix of glass.

ka thousand years.

lapilli pyroclasts between 2 mm and 64 mm.

lava levee ridges along the sides of a lava flow where the center of the lava drained forward at the end of the effusion stage and left the solidified margins standing higher.

lava tube a channel inside a lava flow. Commonly starts out as an open river of lava that becomes covered with a solidified roof as the lava flow advances and cools. Can collapse if lava drains out of the front of the tube, or remain open if the roof is strong enough.

lithology the study of rocks; types of rocks.

Ma mega-annum: million years; the place in geologic time of the age of a rock. The Geologic Time Scale starts at the present (0.0 Ma) and increases back in time to the estimated age of Earth: 4,600 Ma. In comparison, the Christian Calendar starts at the birth of Christ (0.0 years) and increases forward in time to the present (ex. 2022).

matrix supported the character of a geologic deposit where larger fragments are isolated in a mixture of finer-grained material.

monocline a downward bend in a generally horizontal layer of rock.

m.y. million years; an interval of geologic time. For example, if the age of a rock is 30 Ma, the rock formed 30 m.y. ago or the rock is 30 m.y. old.

orogeny a mountain-building event that produces folds and faults by compression forces.

pahoehoe the type of basalt lava flow characterized by ropy, or corded, surface structures. Varieties include massive, slab, entrail, festoon, shelly, and spiny which is transitional to aa.

palagonite an orange to tan substance that forms by the hydrous alteration of basaltic glass; it contains clay and hydrous iron oxide.

paleomagnetic refers to the magnetism of a rock that developed in the past, either when the rock originated or at a later time if the environment changed.

paleovalley a former valley that has been filled by a younger rock or deposit.

Pelêan a type of eruption associated with lava domes and viscous lava when powerful explosions blow lava, rocks, crystals, pumice, and ash several kilometers above the vent. Gravity collapses the eruption column, which then spreads laterally across the ground surface as hot pyroclastic flows that deposit block and ash breccias. Named after a devastating eruption of Mt. Pelêe in 1902 on the Caribbean island of Martinique.

petrography description and classification of rocks.

phaneritic the texture of a rock composed of crystals large enough to distinguish without a lens.

phenocryst a larger crystal set in a matrix of smaller crystals or glass.

polymictic refers to a rock that is made up of other rocks of different types.

protalus rampart a ridge consisting of coarse debris at the downslope edge of an existing or melted snowbank.

pumice frothy glass.

pyroclast a fragment of a rock, lava, pumice, dense glass, or crystal that was broken by a volcanic explosion. Pyroclasts are classified according to size: **ash** < 2 mm; **lapilli** 2-64 mm; **bomb** and **block** > 64 mm.

pyroclastic an adjective that refers to a rock, deposit, or mobile volcanic system (a flow) composed of pyroclasts.

rootless lava flow a lava flow formed by down-slope flow of a deposit of molten bombs and lapilli on or near the summit of a volcano. The components of the flow originated by explosive disruption of lava rather than by direct effusion of coherent lava from a vent, hence "rootless".

Strombolian the type of volcanic eruption characterized by pulsating explosions of lava at intervals of minutes, to hours, to days; typically basalt to basaltic andesite lava. Named after Stromboli volcano in Italy.

strike valley a valley eroded by a river in the direction of the strike, or trend, of tilted strata. The valley is commonly positioned on a soft layer between harder layers. The Little Colorado River flows northwest in a strike valley.

subPlinian the type of volcanic eruption characterized by periods of sustained emission of cinders in a column that might reach as high as 20 km above the vent. Sustained Plinian eruption columns might reach 40 km or more above the vent; named after Pliny the Elder.

tachylite black basaltic glass. Found in cinders and the crusts of basalt lava flows. **Obsidian** is black rhyolitic glass high in silica. Tachylite typically is opaque to light whereas obsidian is translucent in thin pieces.

vesicle a gas pocket in a volcanic rock.

vesicle cylinder a vertical column of closely spaced vesicles in the interior of a basalt lava flow.

vesicle sheet a horizontal layer of closely spaced vesicles in the upper part of a basalt lava flow; cylinders feed sheets.

xenolith a fragment of a "foreign" rock inside a lava flow or other rock of solidified melt.